

THE SMALL-SCALE CLUSTERING PROPERTIES OF DWARF GALAXIES

J. PATRICIA VADER

Yale University Department of Astronomy, Box 6666, New Haven, CT 06511

AND

ALLAN SANDAGE

The Observatories of the Carnegie Institution of Washington, 813 Santa Barbara Street, Pasadena, CA 91101

Received 1991 May 28; accepted 1991 July 8

ABSTRACT

We report two results on the small-scale clustering properties of dwarf galaxies identified in the vicinity of early-type Shapley-Ames galaxies on high-resolution photographic plates.

1. Dwarf galaxies display the same trend of stronger clustering toward earlier morphological type on small scales as their giant counterparts on larger scales. Early-type dwarfs have a surface density as a function of projected radial distance R from E–E/S0 galaxies of the form $\Sigma(R) \propto R^{-1.22 \pm 0.05}$ for $25 < R < 400$ kpc ($H_0 = 50$) which mimicks that of the dark halos of spiral galaxies. It corresponds to a spatial two-point correlation function $\xi(r) = (r/r_0)^{-\gamma}$ with $\gamma = 2.22$ and $r_0 = 10$ Mpc. The steepness of γ and the tendency of early-type dwarf galaxies to be satellites of giant galaxies suggest that early-type dwarf galaxies are the most strongly clustered of all galaxies. Our results indicate that early-type dwarfs can be used as dynamical probes of dark halos around early-type giant galaxies and as tracers of the dynamical evolution of such halos in dense environments.

2. The trend of increasing early-type dwarf frequency per early-type giant with environment richness previously established for rich groups is found to be continued in the less rich environments studied here. Our data cover a range in early-type dwarf to giant ratio of a factor of 20. We find a minimum value of ~ 0.25 for isolated early-type galaxies, as compared to a maximum of ~ 8 previously found in rich environments like the Virgo Cluster.

Subject headings: dark matter — galaxies: clustering

1. INTRODUCTION

Recent studies of clusters and groups of galaxies (Binggeli, Sandage, & Tammann 1985; Ferguson 1990; Ferguson & Sandage 1990; Ferguson & Sandage 1991, hereafter FS91) have shown that the relative frequency of early-type dwarf and giant galaxies is a *monotonically increasing function of the richness of the aggregate*. This phenomenon is different from the morphology-density relation which is obeyed by both giant (Dressler 1980) and dwarf galaxies (Binggeli, Tammann, & Sandage 1987; Ferguson & Sandage 1989). The morphology-density relation combined with (1) an increase of the number ratio of early-type dwarfs to giants with environment richness and (2) a tendency of early-type dwarfs to be satellites of bright galaxies in regions of low galaxy density (Binggeli, Tarengi, & Sandage 1990) suggests that early-type dwarfs are more strongly clustered than their giant counterparts. This may provide a clue to the origin of early-type dwarfs and deserves further attention. In this *Letter* we investigate the small-scale clustering properties of dwarf galaxies in the vicinity of galaxies of type E and E/S0 in the Revised Shapley-Ames Catalog of Bright Galaxies (Sandage & Tammann 1987, hereafter RSA). Our study is based on inspection of large-scale photographic plates centered on the RSA galaxies. We adopt a Hubble constant of $50 \text{ km s}^{-1} \text{ Mpc}^{-1}$.

2. THE DATA

Our source material is the same glass plates that were used for the classification of RSA galaxies. These have been

obtained during the past 80 years, first with the 60 and 100 inch (1.5 and 2.5 m) telescopes on Mount Wilson, then with the Palomar 200 inch (5 m) telescope and finally with the Dupont 100 inch (2.5 m) telescope at Las Campanas until 1985. Preliminary results of a CCD imaging program (Chaboyer & Vader 1991) indicates that the apparent limiting blue magnitude of objects that can be identified as dwarfs on the Palomar and Las Campanas plates (the majority of the material) is $m_{\text{lim}} \sim 18.5$. Although the detection limit is defined by surface brightness rather than total magnitude, these limits are almost equivalent (Binggeli et al. 1990). We have inspected 118 plates centered on E–E/S0 galaxies that are not included in the previously studied groups.

We distinguish four varieties of early-type dwarf galaxies (Sandage & Binggeli 1984): dwarf ellipticals without (dE) and with nuclei (dE, N), dwarf lenticulars (dS0), and compact dwarf ellipticals (cE) of which M32 is a prototype. Late-type dwarfs are referred to here as dI without further distinction. We have assigned to each dwarf one out of three identification confidence levels: certain dwarfs (class 1), probable dwarfs (class 2), and likely background objects (class 3). We caution that class 3 objects do not include all unambiguous background objects but only objects that are likely but not unambiguously background, so that a small fraction of them may be dwarf galaxies. Table 1 shows the number of dwarfs per class for each type. A complete catalog with positions, magnitudes, and morphological types of dwarf galaxies identified in the vicinity of all RSA galaxies will be published separately (Vader & Sandage 1991).

TABLE 1
NUMBER OF DWARFS NEAR E AND E/S0
GALAXIES

TYPE	CLASS		
	1	2	3
dE, N	45	11	} 7
dE	14	18	
dS0	15	3	
cE	9	13	
dI	17	17	24
Total	100	62	31

3. DATA ANALYSIS

3.1. The Small-Scale Clustering Properties of Dwarf Galaxies

Low surface brightness is a unique signature of dwarf galaxies. Using only surface brightness and morphology as criteria, we have cataloged candidate dwarf galaxies without prior knowledge of redshifts of either the candidate or the central RSA galaxy. Subsequent redshift measurements of six of the brightest class 1 and 2 candidate early-type dwarfs and a few published dwarf redshifts show the candidates to be at the same distance as the RSA galaxy (Vader & Chaboyer 1991). In the following we will assume that the dwarfs identified on a given plate are at the same distance as the RSA galaxy at the plate center.

A first assessment of the small-scale clustering properties of the dwarfs is obtained by comparing the fractions of dwarfs of each type with projected distance $R < 100$ kpc from the RSA galaxy. For dwarfs of class 1 and 2 combined, this fraction varies systematically with morphological type. We find dE, N's to be the most clustered objects, followed by dE's, dS0's, and dI's (we exclude cE's from our analysis because the identification of these relatively high surface brightness dwarfs is unreliable). This sequence is what would be expected if dwarf galaxies obey the same clustering properties or morphology-density relation on small scales as observed for their giant counterparts on large scales (Dressler 1980; Postman & Geller 1984; Giovanelli, Haynes, & Chincarini 1986). The late-type class 3 dwarfs are the least clustered of all objects, as expected if they are mostly background galaxies. On the other hand, there is very little difference in the clustering properties of dE, N + dE + dS0 dwarfs of class 1 compared to class 2. These

findings indicate that all class 1 objects, most class 2 objects, and very few class 3 objects are dwarfs. In the following, dwarfs of class 1, 2, and 3 are assigned weights of 1, 0.8, and 0.2, respectively. Late-type dwarfs are too few in number to be considered in more detail. Our further analysis is therefore restricted to dE, N + dE + dS0 dwarfs.

3.2. The Surface Density Distribution of Early-Type Dwarfs

We define $\Sigma(R)$ as the surface density of early-type dwarfs at linear projected distance R from the nearest giant galaxy. In deriving $\Sigma(R)$ from our data, we need to take into account differences in surface area sampling due to the finite plate size and to correct the data for incompleteness at the faint luminosity end. We have binned the dwarfs in seven annuli whose inner and outer radii are given in Table 2. In each bin we have only included those dwarfs found on plates whose effective linear radius satisfies $R_{\text{eff}}(\text{kpc}) = 23.3 (v/4000 \text{ km s}^{-1}) (\theta_{\text{eff}}/1') > R_0(\text{kpc})$, with v the velocity of the nearby RSA giant, θ_{eff} the angular radius of the usable plate area, and R_0 the outer bin radius.

At velocity v we sample dwarfs with absolute magnitude brighter than $M_{\text{lim}} = \min [M_f, m_{\text{lim}} - 5 \log (v/H_0) - 25]$, where $M_f = -13$ is the adopted faint end of the dwarf luminosity function and $m_{\text{lim}} \approx 18.5$ is the plate limit. Assuming that the luminosity function (LF) *per morphological type* is universal (Binggeli, Sandage, & Tammann 1988), we adopt a Schechter function $\phi(M)$ with $M_{B^*} = -17.8$ and $\alpha = -1.35$ which fits Virgo Cluster early-type dwarfs (Sandage, Binggeli, & Tammann 1985). The incompleteness correction is $1/F(v)$, with

$$F(v) = \int_{M_{\text{lim}}(v)}^{-\infty} \phi(M) dM / \int_{M_f}^{-\infty} \phi(M) dM . \quad (1)$$

We have performed the LF corrections to the data in two different ways: (1) as a single correction per bin with v taken to be the median velocity of the associated RSA galaxies in that bin and (2) individual corrections for each dwarf galaxy. For each bin, $\Sigma(R)$ is calculated as the average LF-corrected number of dwarfs per unit surface area per giant galaxy. The results are listed in Table 2 and displayed in Figure 1a. The central deficiency of dwarfs is due to the undetectability of dwarfs against the background light of the giant galaxy and possibly to their destruction by dynamical friction. The two LF correction methods yield very similar densities in the $R = 25$ –

TABLE 2
SURFACE DENSITY OF EARLY-TYPE DWARFS

R BIN (kpc)	N_{giants}^a	v_{median}	$F(v_{\text{median}})$	MEDIAN LF CORRECTIONS		INDIVIDUAL LF CORRECTIONS		
				N_{dwarfs}^b		$\Sigma(R)$ (kpc $^{-2}$)	N_{dwarfs}^b Corrected	$\Sigma(R)$ (kpc $^{-2}$)
				Uncorrected	Corrected			
0–25	110	2630	0.34	4.2	12.4	5.73E–05	7.1	3.31E–05
5–50	109	2630	0.34	21.8	64.2	1.00E–04	63.8	9.93E–05
50–75	108	2645	0.34	17.6	52.2	4.92E–05	56.8	5.35E–05
75–100	101	2665	0.33	19.2	57.5	4.14E–05	53.3	3.84E–05
100–150	82	2980	0.29	20.6	71.7	2.23E–05	74.3	2.31E–05
150–250	62.5	3872	0.19	11.8	62.2	7.92E–06	47.3	6.02E–06
250–400	18	4956	0.11	4.8	41.8	7.59E–06	33.6	6.09E–06
Total number of dwarfs				100.0	362.1		336.2	

^a The total number of giant galaxies whose dwarf companions could be examined over the full range in R of the bin.

^b The total number of dwarfs found in this range of R .

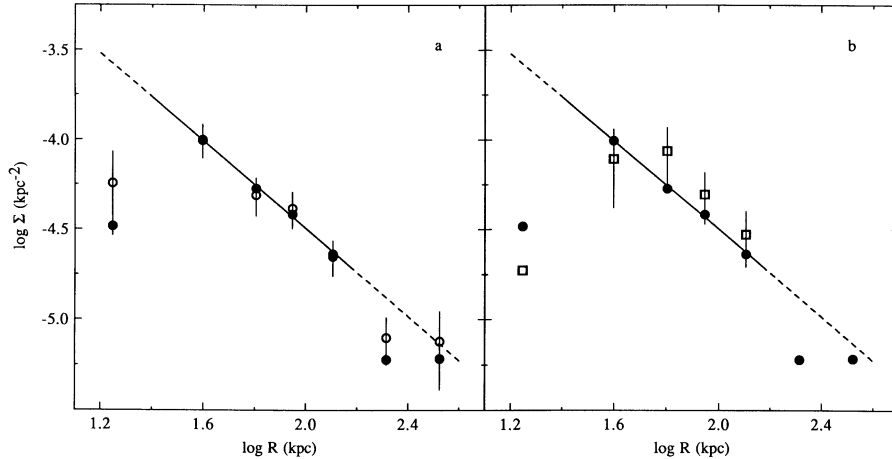


FIG. 1.—(a) The average surface density of dwarfs per giant galaxy $\Sigma(R)$ derived using individual incompleteness corrections (*dots*) and median incompleteness corrections (*open circles and error bars*; the errors are taken to be proportional to the square root of the observed dwarf counts weighted by identification class). The line is a least-squares fit to the data with individual incompleteness corrections in the range $R = 25$ – 150 kpc of the form $\log \Sigma = -1.22 \pm 0.05 \log R - 2.06 \pm 0.10$, with a correlation coefficient $r = 0.998$. (b) The dots and the straight line are the same as in (a). Squares and error bars (derived as in [a]) represent $\Sigma(R)$ for dwarfs in the vicinity of RSA galaxies without bright neighbors within $R \leq 300$ kpc, derived using individual incompleteness corrections.

150 kpc range for which we have the best statistics. A least-squares fit in this range yields a power law of the form $\Sigma(R) = AR^{1-\gamma}$, with $\gamma = 2.22 \pm 0.05$ and a normalization factor A explicitly given in the caption of Figure 1.

3.3. Early-Type Dwarf Galaxies as Probes of Dark Matter

The dwarf density profile derived above more closely follows that of the dark halos of spiral galaxies ($\gamma = 2$, as inferred from flat rotation curves) than that of the luminous halos of either spirals or ellipticals ($\gamma \geq 3$). If on small scales the dwarfs are tracers of the dark matter distribution, a large fraction must be gravitationally bound to the giants. We investigate this on scales ≤ 150 kpc for RSA galaxies selected to have no companion giant galaxy at $R \leq 300$ kpc with luminosity larger than 10% or radius larger than 30% of their own. Forty RSA galaxies satisfy these requirements. A dwarf surface density profile with individual LF corrections is derived for this subset in the same way as above. The results are identical within the errors to those for the whole sample (Fig. 1b). We conclude that independently of environment early-type dwarfs have a density distribution around early-type giants similar to that of dark matter and that they are likely to be gravitationally bound on scales of order 150 kpc. A similar conclusion has been reached by Ferguson (1991) for galaxies in the Virgo Cluster.

3.4. Dependence of the Dwarf Frequency on Environment

The dependence of the dwarf-to-giant number ratio on environment can be quantified by taking the total number of giant E–S0 galaxies, N_g , within a group or cluster as a measure of environment richness. A linear squares fit to the data given for five groups with $N_g \geq 5$ by FS91 yields

$$\log \left(\frac{N_d}{N_g} \right) = 0.50 \pm 0.10 \log N_g - 0.10 \pm 0.14 \quad (r = 0.996), \quad (2)$$

with N_d the total number of early-type dwarfs ($M_B < -13$). We can extend this relation to smaller richness environments by considering the 38 RSA galaxies in our sample that are included in the CfA group survey of Geller & Huchra (1983), 27 of which belong to a group. We determine the LF-corrected

number N_g of early-type galaxies in the groups and adopt $N_g = 1$ for RSA giants not belonging to a group. The LF correction is defined by equation (1). We adopt a LF of the Schechter form with $M_B^* = -20.76$, $\alpha = -0.90$, $\phi^* = 9.18 \times 10^{-4} \text{ Mpc}^{-3}$ for early-type RSA galaxies (Tammann, Yahil, & Sandage 1979), and $M_f = -18$, $m_{\text{lim}} = 14.5$ and the mean CfA group velocity for v . Because the adopted LF represents predominantly giant galaxies, it has a shallower slope α than found for early-type dwarfs or mixed morphology galaxy samples (cf. Binggeli et al. 1988). Differences in surface area sampling due to the finite plate size are taken into account by normalizing the LF-corrected number of early-type dwarfs per giant in each case by the expected average number $\Sigma^*(R_{\text{eff}})$, with R_{eff} the effective linear plate radius as defined above and $\Sigma^*(R)$ given by

$$\Sigma^*(R) = \int_{R_{\text{min}}}^R 2\pi y \Sigma(y) dy = 0.071 \left(\frac{R}{\text{kpc}} \right)^{0.78} - 0.873. \quad (3)$$

A minimum radius of 25 kpc has been taken to account for the strong central deficiency of dwarfs. We have binned our results for giants in the CfA survey according to N_g and computed mean values of N_g and of the *normalized* dwarf-to-giant ratio N_d/N_g and their 1σ standard deviations. Figure 2 shows that, in spite of the large errors due to poor statistics, there is a trend of increasing dwarf-to-giant ratio with environment richness consistent with that found by FS91. Our data cover a range of more than an order of magnitude in $\langle N_d/N_g \rangle$. Field galaxies ($\langle N_g \rangle = 1$) are underabundant in dwarfs by a factor of 10 with respect to the mean of our sample, while the richest groups are overabundant by a factor of ~ 2 . In the region of overlap between our data and those of FS91 we find values of N_d/N_g that are ~ 2.5 times smaller than the actual dwarf-to-giant ratios (eq. [2]). Figure 2 shows the FS91 data points (*crosses*) and equation (2) (*curve*) normalized by a factor of 2.5. The curve is a good fit to our data in the region of overlap and yields somewhat smaller values of $\langle N_d/N_g \rangle$ for $N_g < 5$. The integrated number of dwarfs $\Sigma^*(R)$ becomes equal to 2.5 at $R = 140$ kpc (eq. [3]). This distance is similar to that over which the dwarfs are likely to be gravitationally bound (§ 3.3) and to the radius of ~ 200 kpc of the average projected area

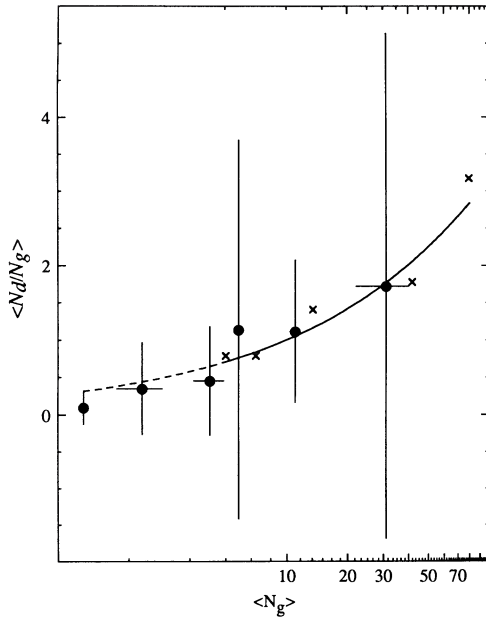


FIG. 2.—The dwarf-to-giant number ratio derived from our data and normalized by the expectation value Σ^* (see text) against the total number of early-type giants in the same CfA group corrected for incompleteness (dots and error bars). The FS91 data points for groups are shown as crosses. The solid curve represents the fit to the FS91 data (eq. [2]) normalized by a mean dwarf to giant ratio of 2.5; the dashed part, an extrapolation to lower richness environments.

occupied per early-type giant in the groups considered by FS91 (their Fig. 3 and Table IX in Ferguson & Sandage 1990). At larger R the integrated number of dwarfs tends to become an overestimate of the “true” N_d/N_g because we have not counted as giants early-type galaxies on the plates that are giants but much fainter ones than the intrinsically bright RSA galaxies. In the following we will adopt 2.5 dwarfs per giant as a representative mean value for all environments.

3.5. The Dwarf-Giant Cross-Correlation Function for Early-Type Galaxies

The clustering properties of galaxies can in general be represented by a two-point correlation function of the form $\xi(r) = (r/r_0)^{-\gamma}$ for $r \ll r_0$, with r_0 the correlation length. For giant galaxies $\gamma = 1.8$ and $r_0 = 10$ Mpc (Peebles 1980). We can derive the values of γ and r_0 describing the small-scale clustering of dwarf galaxies as follows. The dwarf-giant cross-correlation function is given by $\xi(r) = n_d(r)/\langle n_d \rangle - 1$, with $n_d(r)$ the mean dwarf density at distance r from a randomly chosen giant galaxy and $\langle n_d \rangle$ the average spatial density of dwarfs. On the small scales considered here we expect $n_d(r) \gg \langle n_d \rangle$ so that $\xi(r) \approx n_d(r)/\langle n_d \rangle$. Integration of $n_d(r)$ over the line of sight yields the mean surface density of dwarfs $\Sigma(R)$ derived above. Since $\Sigma(R)$ is fitted by a power law, we can use the power-law representation for $\xi(r)$ to obtain the following relation:

$$\frac{\Sigma(R)}{\langle n_d \rangle} \approx r_0 \gamma \int_{-\infty}^{+\infty} \frac{dz}{(R^2 + z^2)^{\gamma/2}} = \beta\left(\frac{1}{2}, \frac{\gamma-1}{2}\right) r_0 \left(\frac{R}{r_0}\right)^{1-\gamma}, \quad (4)$$

where β denotes the beta function. Our power-law fit to $\Sigma(R)$ corresponds to $\gamma = 2.22$ (§ 3.2) and $r_0 = [A/(\beta\langle n_d \rangle)]^{1/\gamma}$. We can obtain a rough estimate of $\langle n_d \rangle$, which is not independently known, from the average giant density and the average number of 2.5 dwarfs per giant. Using the same LF for giants as in § 3.2, we find an average E–S0 giant density of $1.66 \times 10^{-3} \text{ Mpc}^{-3}$. This yields $\langle n_d \rangle = 4.15 \times 10^{-3} \text{ Mpc}^{-3}$ and $r_0 = 10$ Mpc. We

thus find that on small scales, giants are more strongly correlated with dwarfs than with giants, i.e., dwarf galaxies are more strongly clustered than giants. The clustering of giant galaxies systematically increases toward earlier morphological type. The value of γ obtained here for dwarfs is somewhat larger than that of 2.06 for giant E–E/S0 galaxies (Giovanelli et al. 1986). This result and the tendency of early-type dwarfs to be satellites of giant galaxies (Einasto et al. 1974; Binggeli et al. 1990; Vader & Chaboyer 1991) suggest that early-type dwarfs are the most strongly clustered of all galaxies. Data on scales $R > 400$ kpc are needed to confirm this assertion.

4. DISCUSSION

One of the two main results of our new catalog data is that early-type dwarf galaxies are the most clustered of all galaxies and are probably bound to their nearest giant neighbor for separations < 400 kpc. The study of dark halos around early-type giants has so far been restricted to polar ring galaxies (cf. Schweizer, Whitmore, & Rubin 1983; Whitmore, McElroy, & Schweizer 1987) and galaxies with other types of external rings (e.g., Schweizer, van Gorkom, & Seitzer 1989). The similarity of the density profile of the dwarfs studied here to that of dark halos implies that early-type dwarfs can be used as tracers of the dynamical evolution of such halos in dense environments since they would be affected by processes such as tidal stripping (Merritt 1983) in the same way. They are therefore promising new dynamical probes of the dark halos that may exist around early-type giants.

Our second principal result is that the variation of the dwarf-to-giant ratio with environment richness found by FS91 extends to poor groups and isolated galaxies in the general field. This effect cannot be an effect of the morphology-density relation alone because it is also present, though weaker, in the dwarf-to-giant ratio of galaxies of all types (FS91, their Fig. 2). It seems unlikely that environmental effects alone can account for the observed trend. For instance, although competing dynamical effects operate in the right direction, they are too weak. A naive picture would have each giant form with an equal number of dwarf satellites which is subsequently depleted by dynamical friction and tidal stripping. Dynamical friction would destroy dwarf galaxies in poor environments, while in rich environments the stripping of dwarfs along with any extended dark halos by global tidal effects (Merritt 1983) would prevent their destruction and form a general sea of dwarfs in the group or cluster. However, calculations show that, independent of environment, the dwarf population surviving after a Hubble time is the same as the initial population formed at radial distances from the parent larger than 50 kpc, which is contrary to the observations reported here. Other effects such as tidal heating due to galaxy encounters are even less efficient.

For lack of other possibilities, we are left at the moment with the ad hoc explanation that the dependence of the dwarf-to-giant ratio on environment is the result of initial conditions, i.e., the efficiency of forming low-mass galaxies depends on the total mass of the aggregate (a cluster, a group, or an isolated galaxy). Our forthcoming investigation of dwarfs in the vicinity of late-type giants may provide further clues.

J. P. V. is very grateful for the hospitality she enjoyed at The Observatories of the Carnegie Institution of Washington during several short visits which were partially financed by a John F. Enders research assistance grant of Yale University and a small research grant from AAS/NASA.

REFERENCES

- Binggeli, B., Sandage, A., & Tammann, G. A. 1985, *AJ*, 90, 1681
 ———. 1988, *ARA&A*, 26, 509
 Binggeli, B., Tammann, G. A., & Sandage, A. 1987, *AJ*, 94, 251
 Binggeli, B., Tarenghi, M., & Sandage, A. 1990, *A&A*, 228, 42
 Chaboyer, B., & Vader, J. P. 1991, in preparation
 Dressler, A. 1980, *ApJ*, 236, 351
 Einasto, J., Saar, E., Kaasik, A., & Chernin, A. D. 1974, *Nature*, 252, 112
 Ferguson, H. C. 1990, *AJ*, 98, 367
 ———. 1991, *MNRAS*, submitted
 Ferguson, H. C., & Sandage, A. 1989, *ApJ*, 346, L53
 ———. 1990, *AJ*, 100, 1
 ———. 1991, *AJ*, 101, 765 (FS91)
 Geller, M. J., & Huchra, J. P. 1983, *ApJS*, 52, 61
 Giovanelli, R., Haynes, M. P., & Chincarini, G. L. 1986, *ApJ*, 300, 77
 Merritt, D. 1983, *ApJ*, 264, 24
 Peebles, P. J. E. 1980, *The Large-Scale Structure of the Universe* (Princeton: Princeton Univ. Press)
 Postman, M., & Geller, M. J. 1984, *ApJ*, 281, 95
 Sandage, A. S., & Binggeli, B. 1984, *AJ*, 89, 919
 Sandage, A. S., Binggeli, B., & Tammann, G. A. 1985, *AJ*, 90, 1759
 Sandage, A. S., & Tammann, G. A. 1987, *A Revised Shapley-Ames Catalog of Bright Galaxies* (2d ed.; Washington, DC: Carnegie Institution of Washington) (RSA)
 Schweizer, F., van Gorkom, J. H., & Seitzer, P. 1989, *ApJ*, 338, 770
 Schweizer, F., Whitmore, B. C., & Rubin, V. C. 1983, *AJ*, 88, 909
 Tammann, G. A., Yahil, A., & Sandage, A. R. 1979, *ApJ*, 234, 775
 Vader, J. P., & Chaboyer, B. 1991, *PASP*, submitted
 Vader, J. P., & Sandage, A. R. 1991, in preparation
 Whitmore, B. C., McElroy, D. B., & Schweizer, F. 1987, *ApJ*, 314, 439